Proceedings of the
44th IEEE Conference on Decision and Control, and
the European Control Conference 2005
Seville, Spain, December 12-15, 2005

High Efficient Dynamics Calculation Approach for Computed-Force Control of Robots with Parallel Structures

Houssem Abdellatif, Martin Grotjahn and Bodo Heimann

Abstract— **This paper presents a compact and complete approach for realizing high performant control of fully parallel manipulators with a computed-force control scheme (CFC). The proposed method of dynamics computation is based on the principal of virtual power and allows real-time implementation without falling back on inaccurate model simplifications. The efficiency and performance is demonstrated on a 6-dof complex parallel manipulator within commercial control hardware setup. Crucial points for the enhancement of tracking performance are discussed in details.**

I. INTRODUCTION

The majority of commercial robotic systems or machine tools are controlled with simple and linear single-joint feedback controller. The tracking performance is however limited, especially for nonlinear systems in high speed range. There is still a big gap between the sophisticated control algorithms developed in research and the commercial ones. Researcher have to assume though a part of responsibility on this issue, since sometimes the practicability of their developed approaches is neglected. In this paper a computed-force control algorithm (CFC) is carried out for parallel robots from the theory until application on a commercial control system.

It is commonly known that the inverse dynamics computation for feedforward control of robotic manipulators is crucial for high performance tracking [1], [2], [3]. This issue becomes delicate for parallel kinematic manipulators (PKM) since the coupled structure and the high nonlinearity make the dynamics complex to solve [4], [5], [6]. Many approaches were proposed for a computational efficient calculation of the dynamics. We think that there are still different drawbacks. The proof of practicability for control was not regarded in some theoretical works [4], [5], [6], [7]. Besides, most of common approaches neglect friction and joint losses. It was demonstrated in [1] that for some systems, especially friction compensation yields significant improvement of control performance. Successful implementation in robotic systems was shown in [3] and in [8], where friction was taken into account. In the other way around, the rigid-link dynamics were strongly simplified to reduce the computational cost and ensures the real-time ability of the models. In this paper we contribute to remove all these drawbacks by choosing an appropriate approach for modelling and computing the inverse dynamics of parallel manipulators. The proposed model takes into account all relevant dynamics, including inertial influences of all bodies and friction losses in all passive and active joints. The presented approach is kept general and remains available for the major cases of PKM. To assure the computational efficiency and real-time practicability the JOURDAIN's principle of virtual power was regarded for formulating all effects in a uniform way (section II and III). To make the model more powerful and useful for further applications such adaptive control [3] or parameter identification [1], [9], the equations of motion are expressed in a parameter-linear form [6], [10], [11], [12]. The proposed approach is valid and applicable for a wide range of parallel manipulators [2]. The implementation in a real test bed within a commercial control hardware is proved in terms of computational cost and time (section IV) and in terms of control performance (section V). The experimental results are carried out with the innovative direct driven parallel robot PaLiDA. The machine was developed by the institute of production engineering of the university of Hannover for high-speed manipulation and machining [2]. In every section, drawbacks and advantages of alternative methodologies known from literature are critically discussed and systematically compared with the approach proposed in this paper.

H. Abdellatif and B. Heimann are with the Hannover Center of Mechatronics, University of Hannover, Appelstr. 11, 30167 Hannover, Germany. E-mail: {abdellatif,heimann}@mzh.uni-hannover.de

M. Grotjahn is with IAV GmbH, Gifhorn, Germany. E-mail: martin.grotjahn@iav.de

II. KINEMATICS ANALYSIS

A general 6-DOF parallel manipulator is constituted of a moving platform (end-effector platform) attached with six serial actuated kinematic chains to the base platform [2], [4], [5], [6], [7]. Figure 1 shows a general sketch of such robotic manipulator. The goal of the kinematic analysis is the determination of the motions of all modelled bodies in respect to the generalized coordinates. The vector of generalized coordinates $\boldsymbol{\lambda}$ is composed of the cartesian coordinates of the end-effector platform ${}_{(0)}\boldsymbol{r}^{0}_{E} = \left[\begin{array}{ccc} x, & y, & z \end{array}\right]$ and the tilting angles (α, β, γ) according to the cardan or the euler formalism. Additionally, the vector of the generalized velocities is defined as $\dot{\boldsymbol{\theta}} = \left[\begin{array}{cc} {}_{(0)}\boldsymbol{v}_E{}^{\mathrm{T}}, & {}_{(0)}\boldsymbol{\omega}_E{}^{\mathrm{T}} \end{array}\right]^{\mathrm{T}}$ that includes the translational and angular velocities with reference to a cartesian frame. The algorithm efficiency proposed in this paper is based on treating each leg as conventional serial chain. Afterwards the constraints of the closed-loops are taken into account. The vectors joining the fixed joints A_j and the platform joints B_j are

$$ {}_{(0)}\boldsymbol{r}^{A_j}_{B_j} = [x_j \; y_j \; z_j]^{\mathrm{T}} = -{}_{(0)}\boldsymbol{r}^{0}_{A_j} + {}_{(0)}\boldsymbol{r}^{0}_{E} + \boldsymbol{R}^{0E}\,{}_{(E)}\boldsymbol{r}^{E}_{B_j}, \tag{1} $$

0-7803-9568-9/05/$20.00 ©2005 IEEE

where $\boldsymbol{R}^{0E}$ is the orientation matrix of the end-effector (See the sketch in Fig. 1). The velocities and accelerations of B_j are given by

$$\boldsymbol{v}_{B_j} = \boldsymbol{v}_E + \boldsymbol{\omega}_E \times \boldsymbol{r}^E_{B_j}, \tag{2}$$

$$\boldsymbol{a}_{B_j} = \boldsymbol{a}_E + \dot{\boldsymbol{\omega}}_E \times \boldsymbol{r}^E_{B_j} + \boldsymbol{\omega}_E \times \boldsymbol{\omega}_E \times \boldsymbol{r}^E_{B_j}. \tag{3}$$

The single robot struts can be now considered as serial chain robots with respective end-effector kinematics given by $\boldsymbol{r}^{A_j}_{B_j}$, $\boldsymbol{v}_{B_j}$ and $\boldsymbol{a}_{B_j}$. For each body, body-fixed coordinate frames are defined by the modified DENAVIT-HARTENBERG (MDH) notation [13]. This means that the frame i is fixed to the limb i. The $\boldsymbol{z}_i$-axis is the axis of joint i and the $\boldsymbol{x}_i$-axis is the normal of $\boldsymbol{z}_i$ and $\boldsymbol{z}_{i+1}$. Frame i is defined with respect to frame $i-1$ by the homogenous transformation matrix $\boldsymbol{T}_i^{i-1}$

$$\begin{aligned} \boldsymbol{T}_i^{i-1} &= \begin{bmatrix} \boldsymbol{R}_i^{i-1} & {}_{(i-1)}\boldsymbol{r}_i^{i-1} \\ 0\,0\,0 & 1 \end{bmatrix} \\ &= \begin{bmatrix} c_{\vartheta i} & s_{\vartheta i} & 0 & a_i \\ s_{\vartheta i}c_{\alpha i} & c_{\vartheta i}c_{\alpha i} & -s_{\alpha i} & -d_i s_{\alpha i} \\ s_{\vartheta i}s_{\alpha i} & c_{\vartheta i}s_{\alpha i} & c_{\alpha i} & d_i c_{\alpha i} \\ 0 & 0 & 0 & 1 \end{bmatrix} \end{aligned} \tag{4}$$

which is a function of the MDH-parameters ϑ_i, d_i, α_i and a_i [6], [12]. The abbreviations s_x and c_x denote $\sin(x)$ and $\cos(x)$ respectively. The matrix $\boldsymbol{R}_{i-1}^i$ and the vector ${}_{(i-1)}\boldsymbol{r}_i^{i-1}$ define orientation and position of frame i with respect to frame $i-1$. The inverse kinematics of each chain gives an analytic determination of the joint variables ϑ_i (for revolute joints) and d_i (for prismatic joints) as well as their time derivatives. The velocity ${}_{(i)}\boldsymbol{v}_i$ and angular velocity ${}_{(i)}\boldsymbol{\omega}_i$ of each limb i and the corresponding accelerations can be calculated recursively by the following equations:

$$ {}_{(i)}\boldsymbol{v}_i = {}_{(i)}\boldsymbol{v}_{i-1} + {}_{(i)}\tilde{\boldsymbol{\omega}}_{i-1(i)}\boldsymbol{r}_i^{i-1} + \boldsymbol{e}_z\dot{d}_i \tag{5}$$

$$\begin{aligned} {}_{(i)}\dot{\boldsymbol{v}}_i = {}& {}_{(i)}\dot{\boldsymbol{v}}_{i-1} + {}_{(i)}\dot{\tilde{\boldsymbol{\omega}}}_{i-1(i)}\boldsymbol{r}_i^{i-1} + \\ & {}_{(i)}\tilde{\boldsymbol{\omega}}_{i-1(i)}\tilde{\boldsymbol{\omega}}_{i-1(i)}\boldsymbol{r}_i^{i-1} + \ddot{d}_i\boldsymbol{e}_z + \\ & 2\dot{d}_{i\,(i)}\tilde{\boldsymbol{\omega}}_{i-1}\boldsymbol{e}_z \end{aligned} \tag{6}$$

$$ {}_{(i)}\boldsymbol{\omega}_i = {}_{(i)}\boldsymbol{\omega}_{i-1} + \boldsymbol{e}_z\dot{\vartheta}_i \tag{7}$$

$$ {}_{(i)}\dot{\boldsymbol{\omega}}_i = {}_{(i)}\dot{\boldsymbol{\omega}}_{i-1} + \dot{\vartheta}_{i\,(i)}\tilde{\boldsymbol{\omega}}_{i-1}\boldsymbol{e}_z + \ddot{\vartheta}_i\boldsymbol{e}_z \tag{8}$$

where $\boldsymbol{e}_z = [0\,0\,1]^{\mathrm{T}}$. The tilde-operator $\tilde{()}$ defines the crossproduct $\tilde{\boldsymbol{a}}\boldsymbol{b} = \boldsymbol{a} \times \boldsymbol{b}$. The acceleration $\boldsymbol{a}_i$ includes the gravitational acceleration. Simultaneously the translational and rotational Jacobians of each limb can be calculated

$$\boldsymbol{J}_{T_i} = \frac{\partial_{(i)}\boldsymbol{v}_i}{\partial\dot{\boldsymbol{\theta}}} = \boldsymbol{R}_{i-1}^i\left(\boldsymbol{J}_{T_{i-1}} - {}_{(i-1)}\tilde{\boldsymbol{r}}_i^{i-1}\boldsymbol{J}_{R_{i-1}}\right) + \boldsymbol{e}_z\frac{\partial\dot{d}_i}{\partial\dot{\boldsymbol{\theta}}} \tag{9}$$

$$\boldsymbol{J}_{R_i} = \frac{\partial_{(i)}\boldsymbol{\omega}_i}{\partial\dot{\boldsymbol{\theta}}} = \boldsymbol{R}_{i-1}^i\boldsymbol{J}_{R_{i-1}} + \boldsymbol{e}_z\frac{\partial\dot{\vartheta}_i}{\partial\dot{\boldsymbol{\theta}}}. \tag{10}$$

with $\boldsymbol{R}_i^{i-1} = (\boldsymbol{R}_{i-1}^i)^{\mathrm{T}}$. For the actuated joints characterized by the vector of actuated variables $\boldsymbol{q}_{\mathrm{a}}$, the inverse Jacobian of the manipulator $\boldsymbol{J}^{-1} = \partial\dot{\boldsymbol{q}}_a/\partial\dot{\boldsymbol{\theta}}$ can be determined in the same sense. The use of the MDH-notation is advantageous for the analysis of the forward and inverse kinematics. It allows the application of reduction rules for dynamic parameters and ensures the computational efficiency within standard control and processors [12]. Similar conclusions were also met recently for parallel manipulators [6]. Furthermore, the real axis directions of the universal joints can be easily taken into account. The conventional simplification as ball-and-socket joint is not necessary [4], [5].

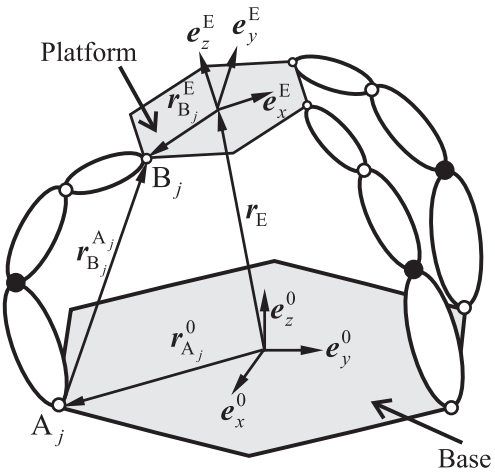

Fig. 1. Scheme of a general 6-DOF parallel manipulator.

III. EFFICIENT DYNAMICS FORMULATION

The dynamics of parallel robots has been formulated in literature mostly using the Newton-Euler formalism, which is more efficient for such mechanisms. To avoid the calculation of constraint forces like in [5] or [7], the D'ALEMBERT principle of virtual work was used in [4], [10]. This principle is based on virtual displacements and virtual work. It is though not appropriate for modelling friction forces that depends however on joint velocities. To assure the integration of friction within the inverse dynamics, the equivalent JOURDAIN's principle of virtual power is used. It considers virtual velocities and virtual power and allows not only efficient calculation but also provides the linear form of the dynamics, necessary for accurate model identification [1], [9]. The power balance equation is obtained as

$$\delta\dot{\boldsymbol{\theta}}^{\mathrm{T}}\boldsymbol{\tau} = \delta\dot{\boldsymbol{q}}_{\mathrm{a}}^{\mathrm{T}}\boldsymbol{Q}_{\mathrm{a}} \Leftrightarrow \boldsymbol{\tau} = \left(\frac{\partial\dot{\boldsymbol{q}}_{\mathrm{a}}}{\partial\dot{\boldsymbol{\theta}}}\right)^{\mathrm{T}}\boldsymbol{Q}_{\mathrm{a}}, \tag{11}$$

where $\boldsymbol{\tau}$ is the vector of the generalized forces and $\boldsymbol{Q}_{\mathrm{a}}$ is the vector of the actuator forces. Equation (11) means that the virtual power resulting in the space of generalized coordinates is equal to the actuation power. The power balance can be applied for rigid-body forces:

$$\boldsymbol{Q}_{\mathrm{a,rb}} = \left(\frac{\partial\dot{\boldsymbol{q}}_{\mathrm{a}}}{\partial\dot{\boldsymbol{\theta}}}\right)^{-\mathrm{T}}\boldsymbol{\tau}_{\mathrm{rb}} = \boldsymbol{J}^{\mathrm{T}}\boldsymbol{\tau}_{\mathrm{rb}}, \tag{12}$$

and for friction losses in all joints

$$\boldsymbol{Q}_{\mathrm{a,f}} = \left(\frac{\partial \dot{\boldsymbol{q}}}{\partial \dot{\boldsymbol{q}}_{\mathrm{a}}}\right)^{\mathrm{T}} \boldsymbol{Q}_{\mathrm{f}} = \boldsymbol{J}^{\mathrm{T}} \left(\frac{\partial \dot{\boldsymbol{q}}}{\partial \dot{\boldsymbol{\theta}}}\right)^{\mathrm{T}} \boldsymbol{Q}_{\mathrm{f}}. \tag{13}$$

It is important to notice that $\boldsymbol{Q}_{\mathrm{a,rb}}$ and $\boldsymbol{Q}_{\mathrm{a,f}}$ present ALL rigid-body forces and ALL friction forces transformed into the actuation space. The formulation of parameter-linear dynamics is discussed in the following subsections.

A. Parameter-linear Form of Rigid-Body Dynamics

The generalized rigid-body forces for a manipulator with N bodies are

$$\begin{aligned}\boldsymbol{\tau}_{\mathrm{rb}} \;=\; \sum_{i=1}^{N} \Big[& \boldsymbol{J}_{T_i}^{\mathrm{T}} \left(m_{i\,(i)}\dot{\boldsymbol{v}}_i + {}_{(i)}\dot{\tilde{\boldsymbol{\omega}}}_i \boldsymbol{s}_i + {}_{(i)}\tilde{\boldsymbol{\omega}}_{i\,(i)}\tilde{\boldsymbol{\omega}}_i \boldsymbol{s}_i \right) \\ & + \boldsymbol{J}_{R_i}^{\mathrm{T}} \left({}_{(i)}\boldsymbol{I}_i^{(i)}\, {}_{(i)}\dot{\boldsymbol{\omega}}_i + {}_{(i)}\tilde{\boldsymbol{\omega}}_i \left({}_{(i)}\boldsymbol{I}_i^{(i)}\, {}_{(i)}\boldsymbol{\omega}_i \right) \right. \\ & \left. + \tilde{\boldsymbol{s}}_{i\,(i)}\dot{\boldsymbol{v}}_i \right) \Big]. \end{aligned} \tag{14}$$

with dynamic parameters of each body i: its mass m_i, its first moment $\boldsymbol{s}_i := [s_{i_x}\; s_{i_y}\; s_{i_z}]^{\mathrm{T}} = m_{i\,(i)}\boldsymbol{r}_{C_i}^{i}$ ($\boldsymbol{r}_{C_i}^{i}$: vector from coordinate frame to centre of mass) and its inertia tensor about the corresponding coordinate frame ${}_{(i)}\boldsymbol{I}_i^{(i)}$. New operators $()^*$ and $()^\diamond$ are defined:

$$\boldsymbol{\omega}_i^* \boldsymbol{I}_i^\diamond := {}_{(i)}\boldsymbol{I}_i^{(i)}\, {}_{(i)}\boldsymbol{\omega}_i, \tag{15}$$

with $\boldsymbol{\omega}_i^* := \begin{bmatrix} \omega_{i_x} & \omega_{i_y} & \omega_{i_z} & 0 & 0 & 0 \\ 0 & \omega_{i_x} & 0 & \omega_{i_y} & \omega_{i_z} & 0 \\ 0 & 0 & \omega_{i_x} & 0 & \omega_{i_y} & \omega_{i_z} \end{bmatrix}$ and

$$\boldsymbol{I}_i^\diamond = [I_{i_{xx}}\; I_{i_{xy}}\; I_{i_{xz}}\; I_{i_{yy}}\; I_{i_{yz}}\; I_{i_{zz}}]^{\mathrm{T}}, \tag{16}$$

which helps the simplification of the generalized rigid-body dynamics [10], [12]:

$$\boldsymbol{\tau}_{\mathrm{rb}} \;=\; \sum_{i=1}^{N} \underbrace{\left[\boldsymbol{J}_{T_i}^{\mathrm{T}}\; \boldsymbol{J}_{R_i}^{\mathrm{T}}\right] \boldsymbol{\Omega}_i}_{\boldsymbol{H}_i} \underbrace{\begin{bmatrix} \boldsymbol{I}_i^\diamond \\ \boldsymbol{s}_i \\ m_i \end{bmatrix}}_{\boldsymbol{p}_i} \tag{17}$$

$$\;=\; [\boldsymbol{H}_1\; \cdots\; \boldsymbol{H}_N] \left[\boldsymbol{p}_1^{\mathrm{T}}\; \cdots\; \boldsymbol{p}_N^{\mathrm{T}}\right]^{\mathrm{T}}, \tag{18}$$

with

$$\boldsymbol{\Omega}_i = \begin{bmatrix} \boldsymbol{0} & {}_{(i)}\dot{\tilde{\boldsymbol{\omega}}}_i + {}_{(i)}\tilde{\boldsymbol{\omega}}_{i\,(i)}\tilde{\boldsymbol{\omega}}_i & {}_{(i)}\dot{\boldsymbol{v}}_i \\ {}_{(i)}\dot{\boldsymbol{\omega}}_i^* + {}_{(i)}\tilde{\boldsymbol{\omega}}_{i\,(i)}\boldsymbol{\omega}_i^* & -{}_{(i)}\dot{\boldsymbol{v}}_i & \boldsymbol{0} \end{bmatrix}. \tag{19}$$

Considering the power balance given by (11) the actuation forces resulting from the rigid-body dynamics can be derived in a linear form:

$$\boldsymbol{Q}_{\mathrm{a,rb}} = \left[\boldsymbol{J}^T \boldsymbol{H}\right] \boldsymbol{p}_{\mathrm{rb}}^*. \tag{20}$$

The dimension of the parameter vector $\boldsymbol{p}_{\mathrm{rb}}^*$ has to be reduced for an efficient calculation and to assure the identifiability of the system [1], [2], [3]. Only few publications treated the parameter reduction for PKM systematically [6], [12], although this issue is crucial for identification or for adaptive control algorithms [1], [3]. Some approaches were presented and implemented successfully in practice, but the considered models are significantly simplified [3], [8]. In the recently published methodology [6], a very good systematic study of parameter reduction of parallel robots is shown, but unfortunately, no practical results were investigated. The proposed algorithm in the following is based on former works for serial and parallel manipulators [6], [11], [12], [13]. The matrices $\boldsymbol{H}_i$ in eq. (17-20) can be grouped in single serial kinematic chains (which are here the legs or struts), such that a recursive calculation:

$$\boldsymbol{H}_i = \boldsymbol{H}_{i-1}\boldsymbol{L}_i + \boldsymbol{K}_i \tag{21}$$

can be achieved. The matrices $\boldsymbol{L}_i$ and $\boldsymbol{K}_i$ are given in [12] and derived in [13] for NEWTON-EULER equations. The first step considers in eliminating all parameters $p_{\mathrm{rb},j}^*$ that correspond to a zero column $\boldsymbol{h}_j$ of $\boldsymbol{H}$, since they do not contribute to the dynamics. The remaining parameters are then regrouped to eliminate all linear dependencies by investigating $\boldsymbol{H}$. If the contribution of a parameter $p_{\mathrm{rb},j}^*$ depends linearly on the contributions of some other parameters $p_{\mathrm{rb},1j}^*, \ldots, p_{\mathrm{rb},kj}^*$, the following equation holds:

$$\boldsymbol{h}_j = \sum_{l=1}^{k} a_{lj}\boldsymbol{h}_{lj}. \tag{22}$$

Then $p_{\mathrm{rb},j}^*$ can be set to zero and the regrouped parameters $p_{\mathrm{rb},lj,\mathrm{new}}^*$ can be obtained by

$$p_{\mathrm{rb},lj,\mathrm{new}}^* = p_{\mathrm{rb},lj}^* + a_{lj}p_{\mathrm{rb},j}^*. \tag{23}$$

The recursive relationship given in (21) can be used for parameter reduction. If one column or a linear combination of columns of $\boldsymbol{L}_i$ is constant with respect to the joint variable and the corresponding columns of $\boldsymbol{K}_i$ are zero columns, the parameters can be regrouped. This leads to the rules which are formulated in [11], [12] and in [13]. The rules can be directly applied to the struts, since they are treated as serial kinematic chains and their coordinate frames are defined with respect to the MDH-convention (section II). For revolute joints with variable ϑ_i, the other MDH-parameters are constant. This means that the 9^{th} , the 10^{th} and the sum of the 1^{st} and 4^{th} columns of $\boldsymbol{L}_i$ and $\boldsymbol{K}_i$ comply with the mentioned conditions. Thus, the corresponding parameters $I_{i_{yy}}$, s_{i_z} and m_i can be grouped with the parameters of the antecedent joint $i-1$. For prismatic joints however, the moments of inertia can be added to the carrying antecedent joint, because the orientation between both links remain constant. For a detailed insight, it is recommended to consider [6] and [13].

The end-effector platform closes the kinematic loop and further parameter reduction is possible. The velocities of the platform joint points $\boldsymbol{B}_j$ and those of the terminal MDH-frames of the respective leg are the same. It results therefore dependencies of energy-functions of the terminal leg body with those of the platform [11]. Their masses can be grouped to the inertial parameter of the platform according to steiner's laws (see section IV and table I).

B. Parameter-linear Form of Friction Dynamics

Commonly friction in robotics is modelled as force characteristics depending on joint velocities $\dot{q}_i$:

$$Q_{\mathrm{f}_i} = [\phi_1(\dot{q}_i) \dots \phi_m(\dot{q}_i)] \, [\alpha_{1i} \dots \alpha_{mi}]^{\mathrm{T}}, \qquad (24)$$

where ϕ_k are elemental functions which can be linear (e.g. viscous damping) and nonlinear (e.g. coulomb or dry friction). Regrouping friction losses in all n joints yields

$$\boldsymbol{Q}_{\mathrm{f}} = \underbrace{[\boldsymbol{D}_1(\dot{\boldsymbol{q}}), \dots, \boldsymbol{D}_m(\dot{\boldsymbol{q}})]}_{\boldsymbol{D}_{\mathrm{f}}} \underbrace{[\boldsymbol{\alpha}_1^{\mathrm{T}}, \dots, \boldsymbol{\alpha}_m^{\mathrm{T}}]^{\mathrm{T}}}_{\boldsymbol{p}_{\mathrm{f}}}, \qquad (25)$$

with

$$\boldsymbol{\alpha}_k^{\mathrm{T}} = [\alpha_{kj}, \dots, \alpha_{kn}], \qquad (26)$$

and

$$\boldsymbol{D}_k(\dot{\boldsymbol{q}}) = \mathrm{diag}\left(\phi_k(\dot{q}_1), \phi_k(\dot{q}_2), \dots, \phi_k(\dot{q}_n)\right). \qquad (27)$$

Applying the JOURDAIN's principle of virtual power as given in eq. (13) leads to the linear form of the resulting friction forces in the actuation space

$$\boldsymbol{Q}_{\mathrm{a,f}} = \left[\boldsymbol{J}^{\mathrm{T}} \left(\frac{\partial \dot{\boldsymbol{q}}}{\partial \dot{\boldsymbol{\theta}}}\right)^{\mathrm{T}} \boldsymbol{D}_{\mathrm{f}}\right] \boldsymbol{p}_{\mathrm{f}}. \qquad (28)$$

The accurate analysis of friction for PKM is mostly not regarded in most publications, especially in those interested in the theoretical derivation of motion equations [4], [6], [7]. The practice reveals the necessity of friction compensation for control improvement, which explains why its consideration took mostly place in control applications [3], [8], rather than in theoretical works. However, in such cases friction is considered only for the drives, whereas losses in passive joints are neglected. This work proposes the interface of this issue by combining accurate modelling with control application. The use of the JOURDAIN's principle allows a uniform derivation of the integral dynamics of parallel manipulators. The practical application of the presented theory is discussed in the following.

IV. APPLICATION ON THE INNOVATIVE HEXAPOD PALIDA.

The considered hexapod PaLiDA is equipped with electromagnetic linear direct drives as actuators. The struts are variable in length. PaLiDA is designed for high-speed handling and machining tasks with low process forces, like deburing. Direct linear drives have several advantages compared to conventional ball screw drives, e.g. reduced mechanical components, no backlash, low inertia with a minimized number of wear parts. Furthermore, higher control bandwidth and extremely high accelerations can be achieved. The linear direct drives were originally designed for fast lifting movements. For use in robotic application, they were enhanced by power (cooling), mechanical design (reducing backlash and friction), position measuring and control. The system was presented at the Hannover industrial Fair in 2001 (Fig. 2).

Fig. 2. The hexapod PaLiDA. Left: presentation in the Hannover industrial Fair, 2001. Right: CAD-Model

A. Kinematics and Dynamics of PaLiDA

The robot is composed of 6 struts and an end-effector platform. Each strut of the hexapod is composed of three bodies as depicted in Fig. 3. Thus, the whole system is modelled with 19 bodies: the movable platform (index E), 6 identical movable cardan rings (index 1), 6 identical stators (index 2) and 6 identical sliders (index 3). Starting from the robot's inverse kinematics given by (1, 2, 3), the inverse kinematics of the single strut can be solved:

$$l_j = \sqrt{x_j^2 + y_j^2 + z_j^2} \qquad (29)$$

$$\alpha_j = \arctan\left(\frac{x_j}{-z_j}\right) \qquad (30)$$

$$\beta_j = \arctan\left(\frac{y_j}{r_j}\right). \qquad (31)$$

where $r_j = \sqrt{x_j^2 + z_j^2}$. The calculation of the velocities and accelerations as well as the Jacobians of the different bodies is achieved recursively according to (5-10). The necessary definitions of the MDH-Parameters for the struts are given in Fig. 4.

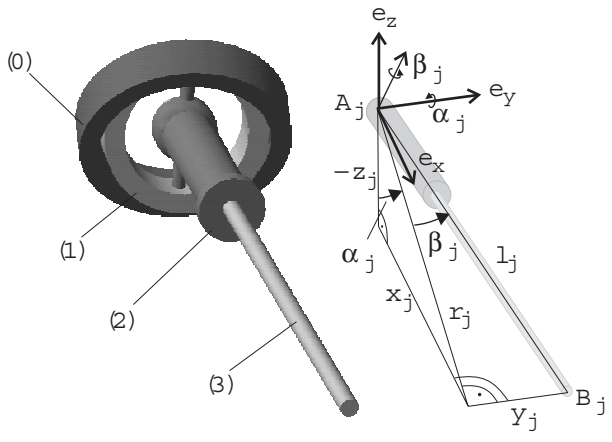

Fig. 3. Kinematics of single strut

For the calculation of the dynamics, minimal base parameters are necessary. For the rigid-body model the rules

i	d_i	θ_i	a_i	α_i
1	0	$\alpha - \frac{\pi}{2}$	0	$\frac{\pi}{2}$
2	0	$\beta - \frac{\pi}{2}$	0	$-\frac{\pi}{2}$
3	l_i	0	0	$-\frac{\pi}{2}$

Fig. 4. MDH-frames and parameters of the struts

discussed in sections III-A are applied. It results a model defined by 10 minimal parameters, which are given in table I. A systematic method for the reduction of friction parameters is not necessary. It is recommended though to examine experimental investigations or system properties to decide about optimal parametrization and modelling. For PaLiDA friction forces in all joints are modelled as a sum of viscous damping and dry friction:

$$Q_{f_i} = r_{1_i}\,\mathrm{sign}(\dot{q}_i) + r_{2_i}\,\dot{q}_i \tag{32}$$

The actuated joints l_j correspond 6 different dry friction and also 6 different viscous damping coefficients. Friction in the the passive joints is modelled only as dry friction with a common parameter for all α_j and another one for all β_j-joints. The friction model contains therefore 14 different parameters. It is possible to keep the maximal number of friction parameters but that would be disadvantageous in terms of parameter identification [1].

TABLE I
BASIC RIGID-BODY MODEL PARAMETERS.

i	p_{rb_i}
1	$I_{zz_1} + I_{yy_2} + I_{zz_3}$
2	$I_{xx_2} + I_{xx_3} - I_{yy_2} - I_{zz_3}$
3	$I_{zz_2} + I_{yy_3}$
4	s_{y_2}
5	s_{z_3}
6	$I_{xx_E} + m_3 \sum_{j=1}^{6}(r_{By_j}^2 + r_{Bz_j}^2)$
7	$I_{yy_E} + m_3 \sum_{j=1}^{6}(r_{Bx_j}^2 + r_{Bz_j}^2)$
8	$I_{zz_E} + m_3 \sum_{j=1}^{6}(r_{Bx_j}^2 + r_{By_j}^2)$
9	$s_{z_E} + m_3 \sum_{j=1}^{6} r_{Bz_j}$
10	$m_E + 6\,m_3$

B. Computational Cost and Model-Parameter Identification

The presented approach is implemented in the computer algebra program MAPLE™. It allows an automatic generation of optimized C-code. The inverse Jacobian given in (12,13) is inverted by Gaussian elimination. The number of operations of the resulting code is given in Table II. The total computational cost proves the efficiency of the approach. As a comparison, the most efficient methodologies known from literature and presented in [6] and in [7] require the total of 2078 and 2150 operations respectively. Regarding that friction was not considered in those approaches, the here discussed algorithm with a total of 1987 operations and including friction can be considered as a further improvement. It is not necessary to parallelize the computation on several processors like suggested in [6], [7], since this can not be fulfilled by commercial and standard control systems. The implementation of the computed-force control on PaLiDA required (including path-planning and joint-control) less that 0.15 ms at a sample rate of 0.5 ms. This excellent real-time property was achieved on a commercial dSPACE Power-PC 604e (333 MHz). The

TABLE II
COMPUTATIONAL COST FOR THE CALCULATION OF DYNAMICS.

	$+/-$	$\times/\div$
Single strut ($6\times$)	88	151
End-effector	100	116
Inversion of $\boldsymbol{J}^{-1}$	137	110
Friction model	36	54
Total	801	1186

presentation of the dynamics in a minimal-parameter form is not only computational efficient but allows also the use of linear estimators for parameter identification [1], [3], [9]. The identification of rigid-body and friction model parameters is necessary for accurate parametrization of the computed-force control. We presented two different strategies for PKM. In [1] the identification of rigid-body and friction models can be achieved separately by using measurements at different configurations. In [9] an optimized harmonic trajectory is used for optimal excitation and identification of the model parameters. In both approaches the motor currents are sufficient for the measurement of the actuator forces. The kinematics are obtained from the actuator lengths measured by internal hall sensors.

V. EXPERIMENTAL RESULTS AND CONTROL IMPROVEMENT

In this section the results of the proposed dynamics modelling methodology is illustrated in terms of control improvement. The concept was implemented on a commercial control hardware with a single processor. First the accuracy of the model prediction in respect to the measured output is investigated. Subsequently the influence of the computed-force in the control improvement is demonstrated. For this purpose a benchmark trajectory is used. It is a circle in the middle of the workspace with an inclination of 30° degrees in respect to the cartesian x-axis. The end-effector velocity is 1 ms^{-1}. It was shown in [3] that for PKM, tracking errors already increase exponentially above a velocity of ≈ 0.1ms^{-1}. Figure 5 shows a comparison between the measured and calculated actuator forces while the benchmark motion for the first 4 - arbitrarily chosen - actuators. Neglecting friction yields important deviation of model-predicted dynamics from the real behavior. Calculation of rigid-body forces is not sufficient. Friction is

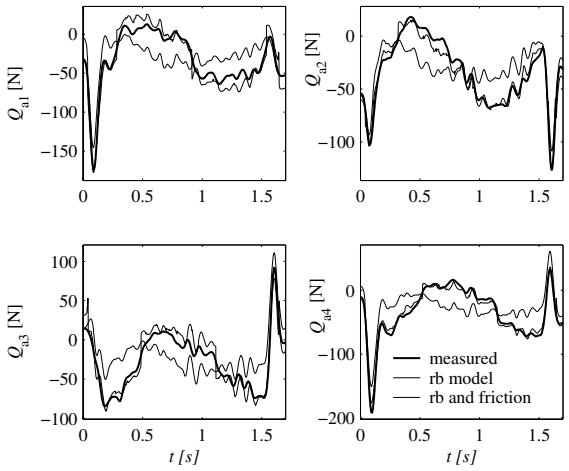

Fig. 5. Comparison between measured and calculated forces by regarding only rigid-body dynamics (rb) and by additionally including friction.

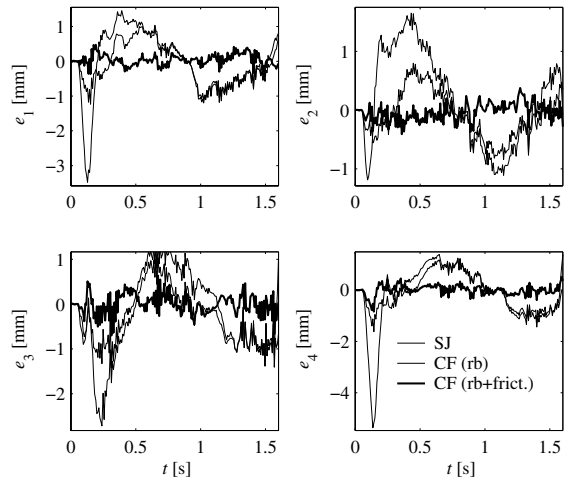

Fig. 6. Control errors of actuators while a circular motion. Comparison between single-joint control (SJ), computed force (CF) using only rigid-body dynamics (rb) and with additional friction compensation (rb+frict.).

crucial for model accuracy. This becomes clear by the comparison of tracking errors when using different models for the computed-force concept. Figure 6 shows control errors for the same actuators by using simple single-joint control (SJ) and computed-force (CF) with only rigid-body dynamics and with additional friction compensation. The experimental results demonstrate primarily, that SJ-control is not appropriate for handling PKM in the range of high speed and high dynamics. The compensation of rigid-body forces yields fair improvement of control quality, mostly in acceleration phases. Most important for the accuracy is the compensation of friction which yields significant reduction of the control errors. This demonstrates exemplarily the decisive role of friction dynamics in control improvement in practice. It is important to mention, that this issue is always close-knit with reliable model identification [1], [9].

VI. CONCLUSIONS

The main idea of this paper is to present a high efficient methodology for the calculation of complex dynamics of parallel manipulators. The proposed approach is based on the JOURDAIN's principle of virtual power and allows a uniform expression for rigid-body and friction dynamics. The resulting computational cost is given and compared to those known from other publications. The method enables real-time calculation and implementation of computed-force control without any model simplifications into standard and commercial control systems. The success was substantiated with experimental results that demonstrate the crucial role of friction compensation for the significant enhancement of control accuracy.

REFERENCES

[1] M. Grotjahn, B. Heimann, and H. Abdellatif, "Identification of friction and rigid-body dynamics of parallel kinematic structures for model-based control," *Multibody System Dynamics*, vol. 11, no. 3, pp. 273–294, 2004.

[2] B. Denkena, B. Heimann, H. Abdellatif, and C. Holz, "Design, modeling and advanced control of the innovative parallel manipulator palida," in *Proc. of the 2005 IEEE/ASME Int. Conference on Advanced Intelligent Mechatronics, AIM2005*, Monterry, USA, 2005, pp. 632–637.

[3] M. Honegger, R. Brega, and G. Schweitzer, "Application of a nonlinear adaptive controller to a 6 dof parallel manipulator," in *Proc. of the 2000 IEEE Int. Conf. on Robotics and Automation*, San Francisco, 2000, pp. 1930–1935.

[4] L.-W. Tsai, "Solving the inverse dynamics of a stewart-gough manipulator by the principle of virtual work," *ASME Journal of Mechanical Design*, vol. 122, no. 5, pp. 3–9, 2000.

[5] K. Harib and K. Srinivasan, "Kinematic and dynamics analysis of stewart pltatform-based machine tool structures," *Robotica*, vol. 21, pp. 541–554, 2003.

[6] W. Khalil and S. D. Guegan, "Inverse and direct dynamics modeling of gough-stewart robots," *IEEE Transactions on Robotics*, vol. 20, no. 4, pp. 754–762, 2004.

[7] C. M. Gosselin, "Parallel computational algorithms for the kinematics and dynamics of parallel manipulators," in *Proc. of the 1993 IEEE Int. Conf. on Robotics and Automation*, New York, USA, 1993, pp. 883–888.

[8] A. Vivas, P. Poignet, and F. Pierrot, "Prediction functional control for a parallel robot," in *Proc. of the 2003 IEEE/RSJ Int. Conference on Intelligent Robots and Systems, IROS2003*, Las Vegas, USA, 2003, pp. 2785–2790.

[9] H. Abdellatif, B. Heimann, and C. Holz, "Time-effective direct dynamics identification of parallel manipulators for model-based feedforward control," in *Proc. of the 2005 IEEE/ASME Int. Conference on Advanced Intelligent Mechatronics, AIM2005*, Monterry, USA, 2005, pp. 777–782.

[10] A. Codourey and E. Burdet, "A body-oriented method for finding a linear form of the dynamic equation of fully parallel robots," in *Proc. of the 1997 IEEE Int. Conf. on Robotics and Automation*, Albuquerque, USA, 1997, pp. 1612–1618.

[11] M. Gautier and W. Khalil, "Direct calculation of minimum set of inertial parameters of serial robots," *IEEE Trans. on Robotics and Automation*, vol. 6, no. 3, pp. 368–373, 1990.

[12] M. Grotjahn, J. Kuehn, B. Heimann, and H. Grendel, "Dynamic equations of parallel robots in minimal dimensional parameter-linear form," in *Proc. of the 14th CISM-IFToMM Symp. on the Theory and Practice of Robots and Manipulators (RoManSy)*, Udine, Italy, 2002, pp. 67–76.

[13] M. Grotjahn and B. Heimann, "Determination of dynamic parameters of robots by base sensor measurements," in *Proc. of the sixth IFAC Symposium on Robot Control (SYROCO)*, Vienna, Austria, 2000.